The Finite Element Method of Flow and Heat Transfer in Heterogeneous Materials

ROSLIANA ESO[1], ARMAN[2]
[1]Department of Physics Education, Universitas Halu Oleo, INDONESIA
[2]Department of Mathematics, Universitas Halu Oleo, INDONESIA

Abstract: - This study aims to explore the heat flow transfer on materials (i.e., homogenous material, particle material, and sandwich material) by using an open-source simulation. The heat flow occurs due to the conduction process equation with the 2T model of the source. We use the Finite Element Method (FEM) to obtain the global heat transfer solution without heat interaction between the walls or layers. The results showed that each domain has a different temperature value according to the point and time used. So further research is expected to research other types of heterogeneous materials.

Key-Words: - Finite Element Method, Heat Flow, particle Material, and sandwich material.

Received: May 19, 2022. Revised: November 16, 2022. Accepted: December 27, 2022. Published: February 7, 2023.

1 Introduction

Recently, there has been a tendency to design the material structure such as composite for a particular application, where various heterogeneities formed from particles or sandwich material are also present due to the manufacturing procedure. Thermal application in heterogeneous materials, [1] range for insulation, heat exchangers, and heat sinks had characterized by the thermal behavior and heat flow processes [2]. Thermal behavior is essential in numerous applications, affecting any device's lifetime and safe operations [3]. The recent experimental findings [4], [5] suggest that heterogeneous materials can show thermal behavior different from Fourier's law at room temperature in a macroscale object due to parallel heat conduction channels. The use of approaches two-temperature model, compared with the experimental data under certain conditions for physical background and characteristic behavior, found that the 2T model offers different insights about the observed heat conduction phenomenon [6].

The difference in the heat conduction channels originates in the heterogeneity. For instance, the homogenous material in a metal sample has good conductivity properties, while the particle material in the inclusions is more similar to an insulator. Assume the modeling that thermal radiation and heat convection could not contribute to the thermal behavior [7].

The two-temperature (2T) approach, [6], [7], [8] however, it has not been tested on heat pulse experiments so far but has a good background and could influence, e.g., the thermoelectric conversion processes [9], [10]. The 2T model has been successfully used for heat transport in metals under ultrashort heat pulses, [11] but they are not tested or not applicable for macroscale solids at room temperature. Furthermore, many other heat equations can be found in the literature [12], [13], [14], but type equations are derived as exceptional cases.

In the present paper, we focus on heat transfer and the thermal characterization of heterogeneous materials, considering only isotropic, heat conduction channels, and constant material parameters using two thermal approaches developed for the materials. We needed the assumption that the initial and boundary conditions can differ from the subsystem and that both subsystems receive different amounts of heat. We also assumed that the heat capacities are equal, and the model needs information about the material structure, especially the constituents. Illustrations or splitting the computational domain into individual small patches and finding local solutions continued on these patches to obtain global heat transfer solutions using the finite element methods (FEM), [15], [16], [17]. However, we need a good command of matrix algebra and computer programming to apply a powerful tool to engineering problems and obtain valuable solutions.

2 Numerical Formulation

In this study, we suppose that the heterogeneous material in heat conduction channels (i.e., particle material and sandwich material) divide into two

subsystems that obey the Fourier law. The system is characterized by two diffusivities, presenting two distinct characteristic time scales. The heat transfer model shows three spatial dimensions as

$$\rho c \frac{\partial T}{\partial t} = -\kappa \nabla^2 T + f(x) \quad x \in \Omega; \tag{1}$$

$$\kappa \frac{\partial T}{\partial x} = q(x) \tag{2}$$

where ρ, c, κ, T, $q(x)$, $f(x)$ are the mass density *(kg/m^3)*, specific heat (*J/kg K*), thermal conductivity (*W/m K*), temperature (*K*) and heat flux (*W/m*) and source term ((*W/m^2*), for the corresponding subsystem, respectively. Moreover, ∂ it denotes the partial derivative concerning time (t) or space (x). If there are no further the source terms $f(x) = 0$, the system will be in the balance of internal energy. The temperature on the boundary of the body is prescribed by $T(x,0) = T_0,\ x = [x_1, x_2] \in \Omega$ where T_0 is a known function, simply a constant. Equation (2) is a constitutive, called Fourier's law. If the heat flux $q(x)$ out of the body (perpendicular to the surface) is determined, then Fourier's law helps us in deciding the partial derivative of the temperature concerning the outward normal vector n: $T = g(x)$; $\kappa \frac{\partial T}{\partial n} = \dot{q}$ For the perfect insulation in Γ_N, the equation becomes a homogeneous Neumann boundary condition $\frac{\partial T}{\partial n} = 0$. Transformation of the model to the non-dimensional system was using the finite element methods (FEM) with assumptions that $\tilde{T} = \frac{T - T_0}{T_0}$, $\tilde{X} = \frac{X}{LR}$, $\tilde{T}(\tilde{x}, 0) = \tilde{T}_0$; $\tilde{x} \in \tilde{\Omega}$, then equation (1) became

$$\frac{\partial \tilde{T}}{\partial t} = \tilde{\kappa} \tilde{\nabla} 2\tilde{T} + \tilde{f}(x);\ \tilde{\kappa} \frac{\partial \tilde{T}}{\partial n} = \tilde{q}(x)\ in\ \Gamma_N;$$
$$\tilde{T} = \tilde{g}(x) \text{ in } \Gamma_D \tag{3}$$

The entire system is characterized by two diffusivities, presenting two distinct characteristic time scales, where a situation can occur in two specific components, such as sandwich material and particle material. The internal heat generation may emerge due to chemical reactions or a heat current flowing through the rod; the left end is kept at a constant temperature, while at the right boundary, no heat is allowed, the source term $\widetilde{(f}(x) = 0)$, the heat exchange between the subsystems and the interface area is uniform in the domain of interest.

Assuming that this functional system is also appropriate for the temperature function T and can express the existence of parallel heat conduction channels, the problem may now be written in the weak formulation and T a solution in the weak sense. For this purpose, we multiply the differential in equation (3) with the so-called test function *v*, which $v \in \tilde{\Omega}$ and $v|_{\Gamma_D} = 0$, and integrate both sides over the whole domain Ω = (0, L). Therefore,

$$.\int_{\tilde{\Omega}} \frac{\partial \tilde{T}}{\partial t} \bullet v\ dA = \int_{\tilde{\Omega}} \tilde{\kappa} \tilde{\nabla}^2 \tilde{T} \bullet v\ dA \tag{4}$$

If we require the test function *v* to satisfy the same Dirichlet boundary condition, $v|_{\Gamma_D} = 0$ as the temperature T, and remember the homogeneous Neumann boundary condition $\frac{\partial \tilde{T}}{\partial n} = 0$, by using the Divergence Theorem, equation (4) becomes

$$\int_{\tilde{\Omega}} \frac{\partial \tilde{T}}{\partial t} \bullet v\ dA = -\int_{\tilde{\Omega}} \tilde{\kappa} \tilde{\nabla} \tilde{T} \bullet \tilde{\nabla} v\ dA +$$
$$\int_{\Gamma_D} \tilde{\kappa} \frac{\partial \tilde{T}}{\partial n} v\ dS + \int_{\Gamma_N} \tilde{\kappa} \frac{\partial \tilde{T}}{\partial n} v\ dS\,. \tag{5}$$

In conduction channels $\int_{\tilde{\Omega}} \frac{\partial \tilde{T}}{\partial t} \bullet v\ dA = -\int_{\tilde{\Omega}} \tilde{\kappa} \tilde{\nabla} \tilde{T} \bullet \tilde{\nabla} v\ dA$, so equation (5) becomes

$$\int_{\tilde{\Omega}} \frac{\partial \tilde{T}}{\partial t} \bullet v\ dA = -\int_{\tilde{\Omega}} \tilde{\kappa} \tilde{\nabla} \tilde{T} \bullet \tilde{\nabla} v\ dA = 0 \tag{6}$$

The first derivative of *v* appears inside an integral. Since the integration provides a smoothing effect, $\dot{v}$ Need to be continuous, so the calculus comes into play for a differentiable function of the weak derivative that is equal to the usual result.

If time discretization was using implicit schema and assuming that $\tilde{T}^k(x) \approx u(x, \kappa\tau)$, $q^k(x) \approx q(x, \kappa\tau)$, and $\frac{\tilde{\boldsymbol{T}}^{\kappa} - \tilde{\boldsymbol{T}}^{\kappa-1}}{\boldsymbol{\tau}} \approx \frac{\partial \tilde{T}}{\partial t}(x, \kappa\tau)$ which τ is time interval $(\tau > 0)$, $\kappa = 1, 2, 3, \ldots n$, the heat transfer model show as

$$\int_{\tilde{\Omega}} \tilde{\boldsymbol{T}}^{\boldsymbol{k}} v\ dA + \tilde{k} \int_{\tilde{\Omega}} \boldsymbol{\tau} \tilde{\nabla} \tilde{T}^k \bullet \tilde{\nabla} v\ dA = \int_{\tilde{\Omega}} \tilde{\boldsymbol{T}}^{\boldsymbol{k-1}} v\ dA \tag{7}$$

where $\int_{\tilde{\Omega}} \tilde{\boldsymbol{T}}^{\boldsymbol{k}} v\ d\tilde{A}$ is a given function and $\int_{\tilde{\Omega}} \tilde{\boldsymbol{T}}^{\boldsymbol{k}} v\ dA + \tilde{k} \int_{\tilde{\Omega}} \boldsymbol{\tau} \tilde{\nabla} \tilde{T}^k \bullet \tilde{\nabla} v\ d\tilde{A}$ An unknown function.

The numerical solution simulation uses FreeFem++ software, an open-source software combined with Gnuplot, to perform a chart. One must define initial and boundary conditions to solve these heat conduction models. In this study, we will restrict the material to three domains (i.e., a homogeneous domain, a particle domain, and a sandwich domain, with a specific boundary surface to make it easier to simulate. Heterogeneous materials define as materials with dramatic heterogeneity in composition from one domain area to another. The domain sizes could range from micrometers to millimeters, and the domain geometry can vary to form very diverse material systems.

One must define the initial temperature distribution and boundary surface for a homogenous domain material model. The boundary conditions are defined through the constitutive equations to preserve physical consistency. In particle material, the subsystems are composed of large-size particles scattered in the material. The boundary conditions do not require special situations, whereas, in sandwich material with a multi-layer domain, each layer has different characteristics, which could be a restrictive property. The field is rectangular on the x-axis and y-axis, as shown in figure1.

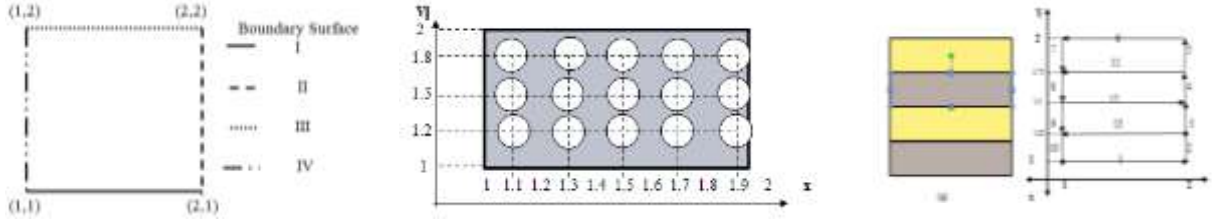

a. Homogen domain b. Particle Domain c. Sandwich Domain

Fig. 1: Illustrating the materials: a. Homogen domain, b. Particle domain, and c. Sandwich domain

First, we need to perform boundary coordinates in the x-y plane, which surface one is on $\binom{x}{y} = t\binom{2}{1} + (1-t)\binom{1}{1}$, surface II on $\binom{x}{y} = t\binom{2}{2} + (1-t)\binom{2}{1}$, surface III on $\binom{x}{y} = t\binom{1}{2} + (1-t)\binom{2}{2}$, and surface IV on $\binom{x}{y} = t\binom{1}{1} + (1-t)\binom{1}{2}$. In FreeFem++ programming, each coordinate point will be generating mesh and connecting each line in a triangle form, for example

```
int n =5.;
border C1(t=0,1){x = 1+t;y=1;label=1;};/Surface I
border C2(t=0,1){x = 2; y=1+t;label=2;};/Surface II
border C3(t=0,1){x = 2-t;y=2;label=3;}; /Surface III
border C4(t=0,1){x = 1; y=2-t;label=4;};/Surface IV
mesh Th = build mesh(C1(n)+C2(n)+C3(n)+C4(n));
plot(Th,ps="mesh.eps");
```

On the particle domain displayed in figure 1, we need to perform 14 circles with a diameter of 0.15; for example, the center point of circle 1 is on $x = 1.1+0.075\cos\theta$ and $y = 1.2+0.075\sin\theta$, circle two on $x = 1.3+0.075\cos\theta$ and $y = 1.2+0.075\sin\theta$, and so forth.

On the other side, for sandwich-structured composite, the domain comprises four layers of material consisting of two types of materials with 13 boundary surfaces. On the x-y plane, surface one is lying on $\binom{x}{y} = t\binom{2}{1} + (1-t)\binom{1}{1}$, or $x = 1+t$ and $y = 1$, surface 2 on $\binom{x}{y} = t\binom{2}{1.25} + (1-t)\binom{2}{1}$, or $x = 2$ and $y = 1+0.25t$, surface three on $\binom{x}{y} = t\binom{2}{1.5} + (1-t)\binom{2}{1.25}$, or $x = 2$ and $y = 1.25+0.25$ t, and so on.

3 Results and Discussion

3.1 Numerical Simulation on Homogeneous Materials

The system has an initial temperature of 0℃; on the top layer at y = 2, the temperature is set at 300℃. Otherwise, at the bottom layer at y = 1, the temperature is set at 20℃. The interval used for iteration time is 0.01. The iteration process starts from t = 0, 0.01, 0.02, up to t = 5. Regarding the boundary conditions, the heat will not come out from the left and the suitable material because that part is the insulin surface which will not penetrate heat and does not transfer heat, so the temperature inside changes faster. The illustration of heat flow in the homogenous material is present in figure 2.

We will consider on three-point where the first point (1.5,1.8), the second point (1.5,1.5), and the third point (1.5,1.2) have the same temperature initial 0^0C at the t = 0. Furthermore, the temperature at the first point, the nearest temperature of 300^0C, has changed at all times, where for 100 times iteration at t = 1, it is 243° C; for 200 times iteration at t = 2, it is 244° C, and at t = 3, t = 4, and t = 5 the temperature value is is the same as when t = 2 which is 244° C. Furthermore, at the second point, the temperature value has changed at each time, t = 1 of 159° C, at time of t =

2 of 160°, and at time of t = 3, t = 4, and t = 5 the value the temperature is the same as when t = 2 which is 160° C. For the third point near the bottom surface with a temperature of 20^0 C, the temperature has changed, where for 100 times iteration at t = 1, the value was 75° C. At 200 times iteration, t=2, its temperature was 76° C and stable not change for t = 3 (300 iterations), t = 4 (400 iterations), and t = 5 (500 iterations).

The dramatic temperature change appears for 0 to 200 times iterations and then tends to be stable. It is clear that along the y-axis, the temperature changes vertically where at the first point, nearest the source at 300 ^{0}C, the temperature was stable at 244 ^{0}C; at the second point, in the middle, the temperature was stable at 160 ^{0}C and the third point, in the bottom nearest temperature 20 ^{0}C, the temperature was steady at 76^{0}C. On the other side, from figure 2, the shape of the heat flow is flat, which shows that the x-axis will have the same temperature at each of the same y-coordinate.

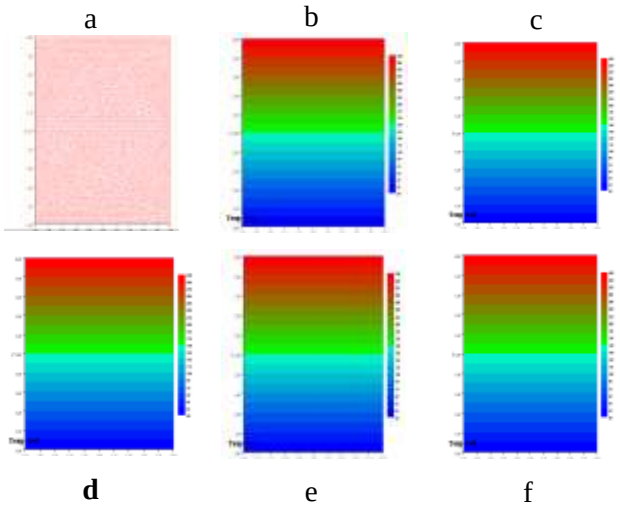

Fig. 2: Temperature distribution on homogeneous materials at different iteration times ; (a) when t = 0, (b) when t = 1, (c) when t = 2, (d) when t = 3, (e) when t = 4, (f) when t = 5

So, we can see for all points, such as points "1.5,1.8, 1.5,1.5, and 1.5,1.2", the temperature only changes for maximal 200 times iteration from t= 0.01 to t = 2, then at t = 3, t = 4, and t = 5 tend to be stable and unchanging as shown by figure 3.

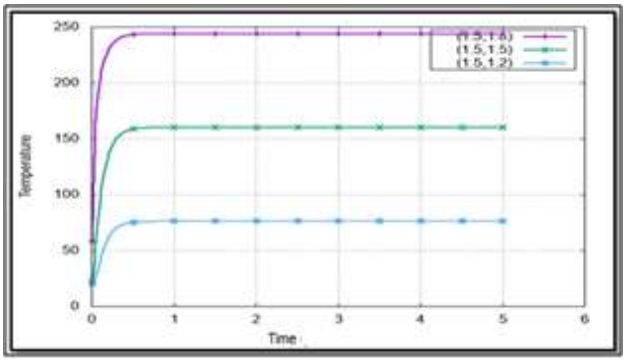

Fig. 3: Temperature graph of the observable point in the homogeneous material simulation

3.2 Numerical Simulation of Particle Material

For particle material, we consider on three-point, the first point (1.4,1.8), the second point (1.4, 1.5), and the third point (1.4, 1.2), which have the same temperature initial 0^0C at the t = 0. After 100 times iteration at t = 1, the temperature at the first point near the heat source 300^{0}C is 247,01^{0}C, in the middle for the second point is 159,751° C, and for the third near the heat source (20 ^{0}C) is 72.728 °C. Furthermore, at 200 times iteration t = 2, the first point temperature is 247.15^{0}C, the second point is 159.997^{0}C, and the third point temperature is 72.857^{0}C. Furthermore, in the next iteration, with t = 3, t = 4, and t = 5, the temperature of the three-point tends to be stable and does not far differ from t = 2, as shown in figure 4.

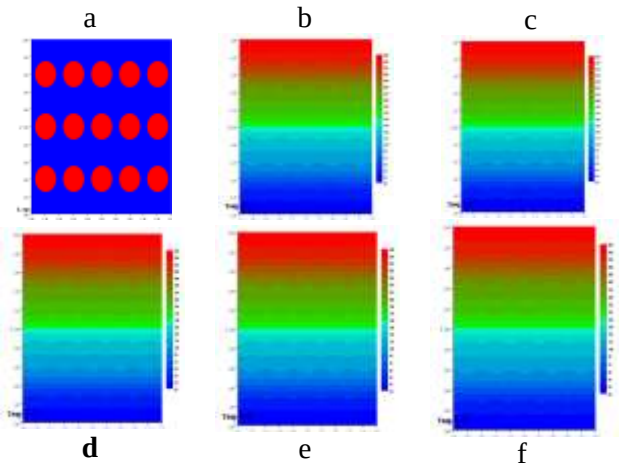

Fig. 4: Temperature distribution on material particles at different times iteration; (a) when t = 0, (b) t = 1, (c) t = 2, (d) t = 3, (e) t = 4, and (f) t = 5

There are differences in the distribution of temperature values at each point reviewed of the particle material compared to the homogeneous material. For the y-axis, the temperature changes

vertically where at the first point, nearest the source at 300 ^{0}C, the temperature was stable at 247.15 ^{0}C; at the second point, in the middle, the temperature was stable at 159.997 ^{0}C, and the third point, in the bottom nearest temperature 20 ^{0}C, the temperature was steady at 72.857^{0}C.

For homogeneous material, the shape of the heat flow is flat. In contrast, for particle material, the heat flow makes a ripple which shows that the x-axis will have different temperatures at each of the same y-coordinate, so they have a different pattern. The temperature of particle material is at a parallel point; however, the difference in temperature values is small enough between points along the x-axis to cause the appearance of small ripples, such as shown in figure 4.

The graphic simulation in figure 3 and figure 5 shows the case that the exact coordinates point has little difference in temperature value for the two sample materials.

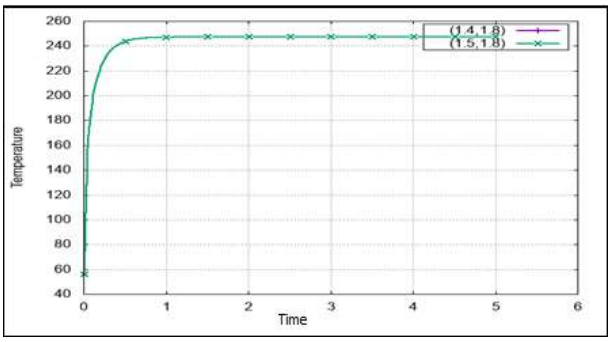

a

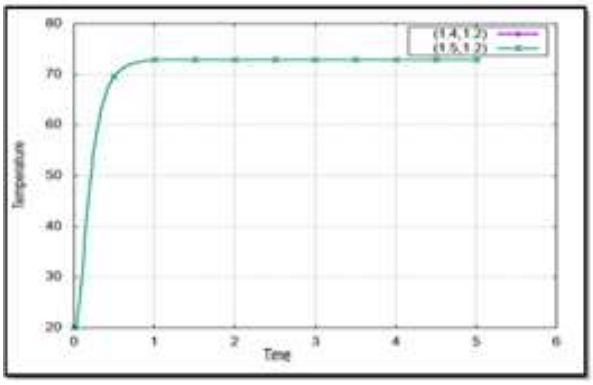

b

Fig. 5: Temperature graph of the observable point in particle material simulation

Considering the two coordinate points (1.4,1.8) and (1.5, 1.8) near the heat source 300^{0}C, only one line appears because overlain both mean almost the same temperature values. Likewise, in coordinates (1.4,1.2) and (1.5,1.2), point near the heat source 20^{0}C, only one line appears because of the overline of the same temperature value. Minor changes to the temperature values along the x-axis are only observed when plotting the data for all points and will appear like ripples, as shown in Figure 4.

3.3 Numerical Simulation on Sandwich Materials

The results of numerical simulations on sandwich materials obtained from the FreeeFEM++ are shown in Figures 6 and 7. For sandwich material, we consider four points where the first point (1.5,1.85), the second point (1.5, 1.65), the third point (1.5, 1.4), and the fourth point (1.5, 1.15) have the same with initial temperature 00C at the t = 0. 100 times iteration at t = 1, the temperature at the review point becomes, the first point at 243.818 ^{0}C, the second at 187.692°C, the third at 122,393°C, and the fourth at 47,906°C. Furthermore, at 200 times iteration, t=2, the temperature increase slightly from t =2, the first point temperature at 244^{0}C, the second point at 187,90C, the third point at 122,66^{0}C, and the fourth point at 47,99°C. Then, in the 300 iterations, t = 3, the first point temperature is 244^{0}C, tends to be the same with t =2, whereas the second point, the third point, and the fourth point, the average temperature rises a little, respectively at 188^{0}C, 122,67^{0}C, and 48°C. For 400 iteration t = 4 and 500 iteration t = 5, the average temperature of all points considered tends to be stable. It does not differ from t=3, as shown in figure 6 and precisely the d section of the illustration.

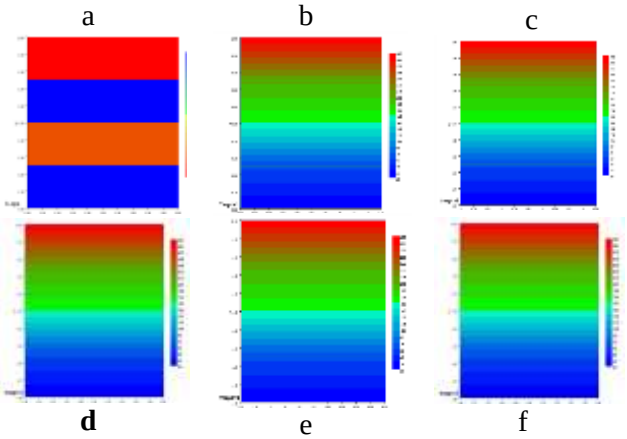

Fig. 6: Temperature distribution on sandwich material at different times; (a) when t = 0, (b) when t = 1, (c) when t = 2, (d) when t = 3, (e) when t = 4, (f) when t = 5.

Based on the selected at the three coordinate points (1.5,1.8), (1.5,1.5), and (1.5,1.2) for the 2T model, which T1at the top of the material is 300°C, and T2 on the bottom is 20°C, both homogenous material and heterogenous material approaches can model the same phenomenon. However, there are

several differences, such as the shape of heat flux and the amount of heat received by each point at the same iteration time. First, with the same initial and boundary conditions, we needed the assumption that all material domains receive the same amount of heat. It appears that from the three points, the homogeneous domain temperature average of point 1 at t = 1s is 247,0060C, t = 2, t = 3, t = 4, and t = 5 at 247.1480C and the material particle domain at t = 1 is 247.010C, t = 2 at 247.150C, t = 3s t = 4s and t = 5 at 247.150C. Successively, the temperature average of point 2 for homogenous material and the material particle domain at t = 1 is 159°C and 159.751°C, t = 2s is 160 °C and 159.9972°C, t = 3s is 160 °C and 159.9973°C when t = 4s is 160 and 159.9974°C, and t = 5s is 160 °C and 159.9975°C. Point 3, the temperature average for homogenous material at time t = 1 is 75°C, at time t = 2, t = 3, t = 4, and t = 5 is 76°C. In contrast, for the material particle domain at time t = 1 is 72.7283°C, at time t = 2 is 72.8566°C, at time t = 3 is 72.85683°C, at time t = 4 is 72.85684°C, and at when t = 5 is 72.85685°C.

With the assumption that the heat capacities are equal, information about the material structure, especially about the constituents, is necessary for heat flux to determine the difference in the heat received due to differences in the composition of the material. Figure 7a, figure 7b, and 7c show where the grey line represents the homogenous material, and the purple line represents the heterogeneous material. It shows that a model should be predictive for practical applications. On designs of composite structures, it is easier to estimate the characteristic time scales using the average temperature model that accommodates the Fourier heat equations. However, creating heterogeneous material would be challenging as it depends on several factors, such as the material structure and a specific heat transfer coefficient for a constituent in the future investigation concerning the presented physical and mathematical aspects.

The graph in figure 7 shows that each point has a different temperature level. It is also clear that the increase in temperature occurs from time t = 0 to t = 1 (iteration 100 times) and towards t = 2 and tends to stable in more than 300 times iterations (t = 3, 4, and 5). From the point observable shown in the graph in fig. 7, the homogenous materials have a uniform temperature along the x-axis. They are also higher than the particle material and the sandwich material.

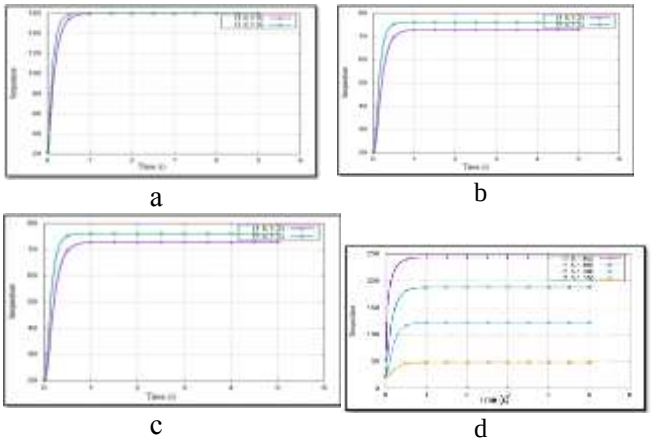

Fig. 7: Temperature distribution of homogenous, particle, and sandwich materials at different times iteration and point coordinates

4 Conclusion

Thermal conductivity of heterogenous and homogenous materials have been successfully simulated using open-source software. The heat flow has several differences, such as the shape of heat flux and the amount of heat each point receives at the exact iteration times. For homogeneous material, the form of the heat flow is flat, while for particle material, the heat flow makes a ripple, so they have a different pattern. The heat flow of sandwich material has distributed horizontally where the temperature change rate maximum only occurs from 0 to 200 times iteration and tends to be the fastest instability. It would be interesting to extend the analysis of temperature efficiency and distribution in both homogenous and heterogenous domain material and the usefulness of a practical system of heat transfer processing

References:

[1] X. Wu and Y. Zhu, "Heterogeneous materials: a new class of materials with unprecedented mechanical properties", *Mater. Res. Lett.*, vol. 5, no. 8, pp. 527–532, 2017.

[2] J. Blackwell, "Microstructure Characterization," *Struct. Form. Polym. Fibers*, pp. 457–520, 2001.

[3] Y. T. Zhu, T. C. Lowe, and T. G. Langdon, "Performance and applications of nanostructured materials produced by severe plastic deformation," vol. 51, pp. 825–830, 2004.

[4] M. Wang, N. Yang, and Z. Y. Guo, "Non-Fourier heat conductions in nanomaterials," *J. Appl. Phys.*, vol. 110, no. 6, 2011.

[5] R. E. Gonzalez-Narvaez, M. López De Haro, and F. Vázquez, "Internal Structure and Heat Conduction in Rigid Solids: A Two-Temperature Approach," *J. Non-Equilibrium Thermodyn.*, vol. 47, no. 1, pp. 13–30, 2022.

[6] R. Kovács, A. Fehér, and S. Sobolev, "On the two-temperature description of heterogeneous materials," *Int. J. Heat Mass Transf.*, vol. 194, 2022.

[7] Y. Hua, and B. Cao, "International Journal of Thermal Sciences Ballistic-diffusive heat conduction in multiply-constrained nanostructures," *Int. J. Therm. Sci.*, vol. 101, pp. XXV–XXV, 2016.

[8] M. Di Domenico, "Nonlocal and nonlinear effects in hyperbolic heat transfer in a two-temperature model," *Zeitschrift für Angew. Math. Und Phys.*, vol. 72, no. 1, pp. 1–15, 2021.

[9] A. A. Abood, K. Amarray, M. Garoum, F. Pirman, and A. Awang, "An extended hot plate method for measurement of thermal conductivity variation with temperature of building materials An extended hot plate method for measurement of thermal conductivity variation with temperature of building materials," 2018.

[10] H. Shibata, A. Suzuki, and H. Ohta, "Measurement of Thermal Transport Properties for Molten Silicate Glasses at High Temperatures by Means of a Novel Laser Flash Technique," vol. 46, no. 8, pp. 1877–1881, 2005.

[11] S. L. Sobolev, and W. Dai, "Heat Transport on Ultrashort Time and Space Scales in Nanosized Systems: Diffusive or Wave-like?," no.15(12), pp. 4287, 2022.

[12] A. Lovas, "Guyer-Krumhansl-type heat conduction at room temperature' 1," pp. 4–7, 2017.

[13] E. P. Scott, M. Avenue, and R. Hall, "The Question of Thermal Waves in Materials," vol. 131, pp. 1–6, 2016.

[14] K. O. V Acs, "Generalized Heat Conduction In Heat Pulse," pp. 1–15, 2014.

[15] I. Erhunmwun, and U. Ikponmwosa, "Review on finite element method," 2018.

[16] Z. Qing, Z. Jiashou, and X. Xiaozhou, "The Partitioned Mixed Model of Finite Element Method and Interface Stress Element Method with Arbitrary Shape of Discrete Block Element," vol. 2013, 2013.

[17] L. Wang, S. Li, G. Zhang, Z. Ma, and L. Zhang, "A GPU-Based Parallel Procedure for Nonlinear Analysis of Complex Structures Using a Coupled FEM / DEM Approach," vol. 2013, no. Iii, 2013.

Contribution of Individual Authors to the Creation of a Scientific Article (Ghostwriting Policy)

The authors equally contributed in the present research, at all stages from the formulation of the problem to the final findings and solution.

Sources of Funding for Research Presented in a Scientific Article or Scientific Article Itself

No funding was received for conducting this study.

Conflict of Interest

The authors have no conflicts of interest to declare that are relevant to the content of this article.